Lidar-Revised Geologic Map of the Wildcat Lake 7.5′ Quadrangle, Kitsap and Mason Counties, Washington

By Rowland W. Tabor, Ralph A. Haugerud, Peter J. Haeussler, and Kenneth P. Clark

Pamphlet to accompany
Scientific Investigations Map 3187

2011

U.S. Department of the Interior
U.S. Geological Survey

U.S. Department of the Interior
KEN SALAZAR, Secretary

U.S. Geological Survey
Marcia K. McNutt, Director

U.S. Geological Survey, Reston, Viginia: 2011

For product and ordering information:
World Wide Web: http://www.usgs.gov/pubprod
Telephone: 1–888–ASK–USGS

For more information on the USGS—the Federal source for science about the Earth,
its natural and living resources, natural hazards, and the environment:
World Wide Web: http://www.usgs.gov
Telephone: 1–888–ASK–USGS

Suggested citation:
Tabor, R.W., Haugerud, R.A., Haeussler, P.J., and Clark, K.P., 2011, Lidar-revised geologic map of the Wildcat Lake 7.5' quadrangle, Kitsap and Mason Counties, Washington: U.S. Geological Survey Scientific Investigations Map 3187, scale 1:24,000, 12 p., and GIS data, available at http://pubs.usgs.gov/sim/3187/.

Contents

Figures

This page intentionally left blank

Introduction

This map is an interpretation of a 6-ft-resolution (2-m-resolution) lidar (light detection and ranging) digital elevation model combined with the geology depicted on the Geologic Map of the Wildcat Lake 7.5′ quadrangle, Kitsap and Mason Counties, Washington (Haeussler and Clark, 2000). Haeussler and Clark described, interpreted, and located the geology on the 1:24,000-scale topographic map of the Wildcat Lake 7.5′ quadrangle. This map, derived from 1951 aerial photographs, has 20-ft contours, nominal horizontal resolution of approximately 40 ft (12 m), and nominal mean vertical accuracy of approximately 10 ft (3 m). Similar to many geologic maps, much of the geology in the Haeussler and Clark (2000) map—especially the distribution of surficial deposits—was interpreted from landforms portrayed on the topographic map. In 2001, the Puget Sound lidar Consortium obtained a lidar-derived digital elevation model (DEM) for Kitsap Peninsula including all of the Wildcat Lake 7.5′ quadrangle. This new DEM has a horizontal resolution of 6 ft (2 m) and a mean vertical accuracy of about 1 ft (0.3 m). The greater resolution and accuracy of the lidar DEM compared to topography constructed from air photo stereo models have much improved the interpretation of geology in this heavily vegetated landscape, especially the distribution and relative age of some surficial deposits. Many contacts of surficial deposits are adapted unmodified or slightly modified from Haugerud (2009). For a brief description of lidar and this data acquisition program, see Haugerud and others (2003).

Base Map Issues

The positions of geographic features on the old contour base of the Wildcat Lake quadrangle compared to the same features on the DEM are displaced by as much as 1,000 ft (300 m). For this reason, contacts adopted directly from Haeussler and Clark (2000) are shown as approximately located. We reproduced structural data and locations of dikes directly from Haeussler and Clark (2000) but moved a few locations slightly to accommodate the revised base map.

No digital depiction of stream or road locations that adequately matches the DEM exists, so we digitized both from the DEM. Many logging roads that are visible on the DEM may not be maintained and are not shown on other large-scale road maps. Consequently, we primarily referred to 1:100,000-scale road depictions and Google Earth to select roads that are shown on this map. We selected rivers and streams to digitize based on drainage shown on the Wildcat Lake 1:24,000 topographic map.

Lineaments

We have shown several conspicuous northeast-trending topographic lineaments on Gold Mountain, mostly in massive Eocene subaerial basalt flows (Tcb) with moderate southwest dips. The westernmost of these lineaments is, in part, coincident with an originally mapped contact between the subaerial basalt (Tcb) and submarine basalt (Tcbs). We have shown this lineament to be a probable fault.

Geologic Units

We did no additional field work to make this revised map. We revised the extent of bedrock outcrops based on geomorphic interpretation of the DEM. We accepted most of the original interpretations of the bedrock geology. We refined locations for a few lengthy buried faults and moved them slightly to accommodate changes in the bedrock extent. Based on recently aquired geophysical data (A.P. Lamb, written commun., 2010), we relocated the buried Seattle Fault.

We extensively reinterpreted contacts, stratigraphy, and age (geologic time scale of Gradstein and others, 2004) of unconsolidated deposits. Our additional mapping is explained in the Description of Map Units and in the discussion in the Surficial Geology section. Much of the text is adapted from Haeussler and Clark (2000).

Cross Section

The topographic profile for the cross section A–A′, as well as contacts of revised units, has been redrawn to match the DEM. We copied the interpretation of subsurface bedrock directly from Haeussler and Clark (2000), except on the north end where the shift in position of the Seattle Fault required interpretive changes.

Previous Work

Geologic mapping within and adjacent to the quadrangle began with Willis (1898) and Willis and Smith (1899), who described glacial deposits in Puget Sound. Weaver (1937) correlated volcanic rocks in the quadrangle to the Eocene Metchosin Volcanics on Vancouver Island. Sceva (1957), Garling and others (1965), and Deeter (1978) all focused on mapping and understanding the Quaternary stratigraphy of the Kitsap Peninsula, but they also examined bedrock in the quadrangle. Reeve (1979) was the first to examine the igneous rocks on Green and Gold Mountains in some detail. Clark (1989) mapped soon after extensive logging on the mountains and, with greater rock exposure, significantly improved Reeve's work.

Yount and Gower (1991) published a bedrock geologic map of the Seattle quadrangle, which includes the Wildcat Lake 7.5′ quadrangle. Yount and others (1993) published a surficial geologic map of the Seattle 30′ by 60′ quadrangle.

Haeussler mapped the surficial geology in the spring and summer of 1998 and in the winter of 1999. Haeussler and Clark (2000) combines Haeussler's mapping and Clark's (1989) essentially unchanged mapping. Haugerud (2009) mapped geomorphic units of about 90 percent of the Wildcat Lake quadrangle as part of a regional geomorphic map of Kitsap County; much of his mapping is incorporated here.

Acknowledgments

We thank Derek Booth and Elizabeth Barnett for very helpful reviews, and we gained much from discussion with Trevor Contreras, Andy Lamb, Jeff Tepper, and Ray Wells.

Geologic Summary

Regional Geologic Setting

The Wildcat Lake quadrangle lies in the forearc of the Cascadia Subduction Zone, about 15 mi (20 km) east of the Cascadia accretionary complex exposed in the Olympic Mountains (Tabor and Cady, 1978b) and about 60 mi (100 km) west of the axis of the Cascades Volcanic Arc. The quadrangle lies near the middle of the Puget Lowland, which typically has elevations less than 600 ft (180 m), but on Gold Mountain, in the center of the quadrangle, elevation rises to 1,761 ft (537 m).

Rocks of the Coast Range basalt terrane that extends from southern Oregon to southern Vancouver Island are exposed on Green and Gold Mountains. This terrane consists of Eocene submarine and subaerial tholeiitic basalt of the Crescent Formation, which probably accreted to the continental margin in Eocene time (Snavely and others, 1968). The Coast Range basalt terrane may have originated as an oceanic plateau or extruded during oblique marginal rifting (Babcock and others, 1992), but its subsequent emplacement history is complex. In southern Oregon, onlapping strata require accretion to have occurred by 50 Ma (Wells and others, 1984). However, studies on southern Vancouver Island suggest that accretion to North America occurred sometime between 42 and 24 Ma (Brandon and Vance, 1992).

After emplacement of the Coast Range basalt terrane, the Cascadia accretionary complex, exposed in the Olympic Mountains west of the quadrangle, developed when younger marine sedimentary rocks were thrust beneath the older basalt terrane (Tabor and Cady, 1978b; Clowes and others, 1987). Domal uplift of the accretionary complex beneath the Olympic Mountains initiated after ~18 m.y. (Brandon and others, 1998).

The Seattle Basin, part of which lies to the north of Green Mountain, may have begun to develop in late Eocene time due to flexural subsidence forced by displacement along the Seattle Fault Zone (Johnson and others, 1994); however, ten Brink and others (2002) suggest motion on the Seattle Fault, and flexural subsidence of the Seattle Basin did not begin until mid-Miocene time.

The Puget Lobe of the Cordilleran Ice Sheet covered the quadrangle during the Vashon stade of the Fraser Glaciation of Armstrong and others (1965). Two-thirds of the quadrangle is underlain by deposits of this glaciation, which lasted from about 15 ka to 13 ka.

Location of the Seattle Fault

Geophysical studies and regional mapping indicate that the Seattle Fault lies north of Green Mountain. This fault produced a large earthquake about 1,100 years ago and may pose a significant earthquake hazard to the Seattle-Tacoma urban area (Bucknam and others, 1992; Atwater and Moore, 1992; Karlin and Abella, 1992; Schuster and others, 1992; Jacoby and others, 1992; Pratt and others, 1997; Blakely and others, 2002; A.P. Lamb, written commun., 2010).

The field mapping by Haeussler and Clark (2000), however, revealed no evidence of Holocene faulting in the Wildcat Lake quadrangle. Projection from known surface ruptures east of the quadrangle, geophysical data (Blakely and others, 2002), and seismic reflection profiles (A.P. Lamb, written commun., 2010) allow the likely position of the Seattle Fault within the Wildcat Lake quadrangle to be defined fairly closely. The lidar DEM shows no fault scarps in the vicinity of the fault. A broad warp of a Vashon-age glacial outwash terrace south of the projected fault location suggests that the Seattle Fault is active at depth but does not reach the surface. See the discussions in the sections on Unconsolidated Deposits and Structural History.

Stratigraphy

Tertiary Bedrock

Lithology, chemistry, and age led Clark (1989) and Haeussler and Clark (2000) to assign the volcanic and volcaniclastic rocks of Green and Gold Mountains to the Crescent Formation exposed on the Olympic Peninsula to the northwest, west, and southwest (Arnold, 1906; Tabor and Cady, 1978a). Clark (1989) compared subaerial volcanic rocks of the Crescent Formation on Green and Gold Mountains (unit Tcb) to the lower and upper Crescent Formation on the Olympic Peninsula. The average subaerial flow thickness of about 30 ft (9 m) at Green and Gold Mountains is thinner than in measured sections of the Crescent Formation on the flanks of the Olympic Mountains, where flows measure 100–200 ft (30–50 m) thick. Vesicles in basalt in the Green and Gold Mountains area are much larger (3 in [7 cm]) than the largest vesicles (<2 in [4 cm]) in the Crescent Formation in the measured sections. Both rock units are subalkaline and tholeiitic, and both have minor and trace elements that plot in the same fields on discriminant diagrams.

The rock column exposed on Green and Gold Mountains, referred to as the “Bremerton rocks” by Clark (1989), is simlar to an ophiolite sequence: from bottom to top, basal gabbro, a locally sheeted dike complex, submarine basalts and volcaniclastic rocks, and subaerial basalt flows. Clark (1989) found more than 200 ft (60 m) of basal leucogabbro and pegmatoid (unit Teg). The upper part of this unit is intruded by numerous diabase and basaltic dikes, which Clark (1989) mapped separately (unit Tegd). The overlying sheeted dike complex is approximately 500 ft (150 m) thick and entirely consists of dikes of diabase and basalt (unit Ted). The submarine volcanic unit (Tcbs) consists of basalt flows interbedded with basaltic sandstone, siltstone, tuffs, and basaltic breccia. Overlying the submarine volcanic unit, subaerial basalt flows (unit Tcb) are more than 600 ft (180 m) thick. Trace-element data from these intrusive and extrusive rocks are similar, which suggests that they are related (Clark, 1989).

Clark (1989) indicated that the sequence differs from an idealized ophiolite stratigraphy in several important ways: (1) it lacks a basal ultramafic complex, (2) the Green and Gold Mountain dike complex has a thickness of about 500 ft (150 m) in contrast to more than 0.5 mi (~1 km) of sheeted dikes in typical oceanic crust, (3) the dikes are not ubiquitously sheeted, and (4) the Green and Gold Mountain sequence is capped by subaerial basalt, whereas most ophiolites are overlain by deep marine sediments. Clark (1989) found that the geochemistry of the gabbro and basalts is transitional between normal mid-ocean-ridge basalt (MORB) and enriched oceanic island basalt.

Preliminary modeling of aeromagnetic and gravity data over Green and Gold Mountains (Haeussler and others, 2000) indicates highly magnetic, dense rocks within a few kilometers of the surface beneath Green and Gold Mountains. A basal ultramafic complex may lie beneath Clark's (1989) Bremerton rocks. Despite the differences between the Green and Gold Mountains rocks and ophiolites, the presence of the dike section on Green and Gold Mountains and the overall similarity to ophiolite layering indicate that this quasi-ophiolite formed in an extensional environment.

Duncan (1982) dated samples from three basalt flows along the northwest shore of Sinclair Inlet, southeast of Bremerton and east of the Wildcat Lake quadrangle. Whole-rock K-Ar ages range between 43.3±0.5 and 49.2±0.6 Ma. However, two of the samples, re-analyzed with the $^{40}Ar/^{39}Ar$ method, yielded whole-rock total-fusion ages of 51.7±2.4 and 55.3±3.1 Ma. Duncan (1982) also step-heated a whole-rock split that produced a 55.4±3.2 Ma age. Two $^{40}Ar/^{39}Ar$ total-fusion ages on one sample of leucogabbro are 50.4±0.6 Ma and 49.2±0.8 Ma (Clark, 1989). Zircon from leucogabbro (unit Teg) at the base of Green Mountain has a $^{206}Pb/^{238}U$ age of 50.5±0.6 Ma (early Eocene; Haeussler and others, 2000). This precise zircon age provides a useful younger limit for the age of the Crescent Formation in this area.

These geochronologic results are consistent with fossil ages from elsewhere in northwestern Washington, which indicates that the Crescent Formation is as old as 53 Ma and is unlikely to be younger than 46 Ma. Calcareous nannoplankton from sedimentary rocks interbedded with submarine basalt at Bon Jon Pass, 33 km northwest of the Wildcat Lake quadrangle, were referred to zone CP11 (about 53 Ma, see Gradstein and others, 2004) by D. Bukry (written commun., 1998; in Tabor and others, 2011). In the Uncas 7.5′ quadrangle, east of Bon Jon Pass, subaerial basalts of the Crescent Formation are overlain by Aldwell Formation that contains benthic foraminifera and mollusks of upper Ulatisian to lower Narizian ages (Spencer, 1984). East of the Uncas quadrangle, submarine deposits of the Crescent Formation have Ulatisian-age foraminifera (Yount and Gower, 1991). Prothero (2001) reports that the base of the Ulatisian may be as old as 51 Ma and that the top of the Ulatisian may be as young as 46 Ma. Gradstein and others (2004) place the early to middle Eocene (Ypresian-Lutetian) boundary at 48.6 Ma.

Dacite dikes (unit Tad, purple dike symbol on map) are the youngest bedrock unit. These dikes cut all other rock units. Clark (1989) reported geochemical data from one sample that has extremely low Ti, low P, high Zr relative to Nb, and very low Cr. This trace-element signature is consistent with a high degree of partial melting. Clark (1989) concluded, based on this chemistry and crosscutting relations, that the dikes are not related to the other rock types on Green and Gold Mountains. More recent work (Tepper and others, 2004) confirms Clark's conclusions. The dikes are adakites (hornblende dacites) that are evidently associated with a subduction regime that preceded establishment of the modern Cascade Volcanic Arc. $^{40}Ar/^{39}Ar$ dating of dike samples by the New Mexico Geochronology Research Laboratory (Esser, 2003) produced ages of 47.8±0.4 and 46.6±1.4 Ma.

Unconsolidated Deposits

Glacial and Interglacial Deposits

Pre-Vashon stade deposits are not shown on this map, but geologic mapping in the Holly 7.5′ quadrangle to the west, by Trevor Contreras (written commun., 2011) of the Washington Department of Natural Resources, Division of Geology and Earth Resources, indicates that older glacial deposits are exposed in Stavis Creek valley in the northwest corner of the Wildcat Lake quadrangle. Similar pre-Vashon stade deposits are probably exposed in the canyon of Big Beef Creek, northeast of Lake William Symington.

Deposits of the last glaciation—the Vashon stade of the Fraser glaciation of Armstrong and others (1965)—surround the Tertiary bedrock highs of Green and Gold Mountains. The Vashon ice sheet first covered the study area about 17,400 cal yr B.P., reached its maximum extent around 16,950 cal yr B.P. (Porter and Swanson, 1998), and covered the area with as much as 3,000 ft (900 m) of ice (Booth, 1987).

As the ice sheet advanced south of Port Townsend, it blocked northward drainage from the Puget Lowland and formed proglacial lakes that drained southward into the Chehalis River and then to the Pacific Ocean. There are no outcrops of the sediments deposited in these advance lakes within the quadrangle, even among the lowest exposures along Big Beef and Stavis Creeks. However, we infer that clay that was encountered in boreholes at the Olympic View Sanitary Landfill, south of Barney White Ranch along the southeast edge of the quadrangle, was deposited as proglacial lake sediments of early Vashon age. This clay lies approximately at sea level and is overlain by sandy and gravelly advance outwash (unit Qva) deposited by streams issuing from the front of the advancing ice sheet. Excellent exposures of advance outwash can be seen along a road leading down to Big Beef Creek northwest of Wildcat Lake. A foreset-topset transition is visible several meters above the level of the creek. Farther up the section, sand and gravel was deposited as debris flows that show poor to no sorting but a weak alignment of clasts. The percentage of cobbles in the debris flows appears to generally increase up section.

Till (unit Qvt) mantles most upland surfaces and marks the presence of the ice sheet in the study area. Till on Green Mountain reaches elevations up to 1,350 ft (410 m). Ice overrode both Green and Gold Mountains, rounding the mountain tops and scouring deep grooves. Green and Gold Mountains also deflected the ice sheet. Linear ridges and grooves on the till plain north and northwest of the mountains trend southwest, but farther east they tend to fan eastward. These trends are more obvious on a regional scale than on the Wildcat Lake quadrangle (see Haugerud, 2009). South of the mountains, the glacial grooves fan east and west, demonstrating the diversion of ice flow around the massif. Granitic clasts within the till attest to a source at least 95 mi (150 km) north in the Coast Mountains of British Columbia.

The Puget lobe rapidly retreated from its maximum extent, leaving the Wildcat Lake quadrangle ice free by about 16,500 cal yr B.P. (Porter and Swanson, 1998). Consideration of likely ice-surface slopes and the distribution of outwash and ice-contact features allow us to outline successive margins of the receding ice (fig. 1). During ice retreat, a series of recessional proglacial lakes formed. The largest of these, ancient glacial Lake Russell (Bretz, 1913), drained south to the Chehalis River (Thorson 1979, 1980; Waitt and Thorson, 1983). Silt and clay (unit Qvrl) near the Union River was deposited in Lake Russell. At least 20 large deltas were built out into Lake Russell (Thorson, 1980), and one of these deltas is located in the southeastern part of the map area. A foreset-topset transition within these recessional outwash sands and gravels (unit Qvru1) at a

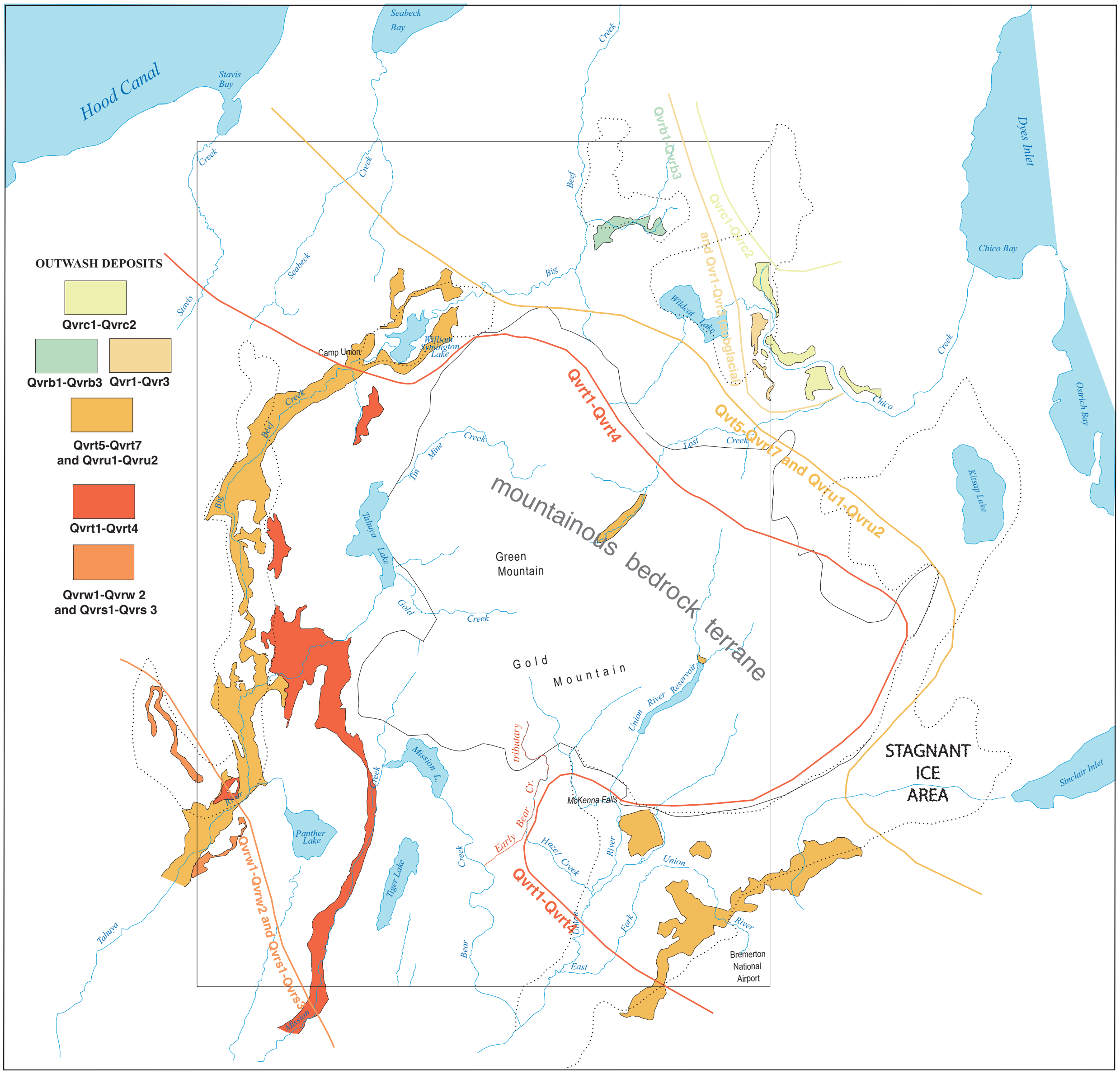

Figure 1. Map showing positions of Puget Lobe termini (heavy colored lines) during deposition of terraces graded to Pleistocene Lake Russell. Dotted lines outline areas of ice-contact features indicating stagnant ice. Terraces and stagnant ice shown beyond the Wildcat quadrangle boundary (solid black outline) are generalized from Haugerud (2009). Qvrw1–Qvrw2, west, probably subglacial, outwash units 1–2; Qvrs1–Qvrs3, southwest, possibly subglacial, outwash units 1–3; Qvrt1–Qvrt4, recessional outwash in higher terraces of Tahuya River and Big Beef and Mission Creeks, Big Beef-Tahuya-Mission outwash units 1–4; Qvrt5–Qvrt7, recessional outwash in lower terraces of Tahuya River and Big Beef Creek, Tahuya River outwash units 5–7; Qvru1–Qvru2, recessional outwash terraces in Union River area, Union River outwash units 1–2; Qvrb1–Qvrb3, recessional outwash terraces above lower Big Beef Creek, Big Beef Creek outwash units 1–3; Qvr1–Qvr3,recessional, probably subglacial, outwash deposits south of Wildcat Creek, outwash units 1–3; Qvrc1–Qvrc2, recessional outwash deposits along Chico Creek, Chico Creek outwash units 1–2.

quarry near McKenna Falls indicates that the shoreline elevation of Lake Russell at the time of deposition was 314 ft (95.7 m) (Thorson, 1989). Because of subsequent glacioisostatic rebound, the former shoreline is probably at higher elevations farther north. Haeussler and Clark (2000) indicate that the contact between the recessional lake deposits (unit Qvrl) and the deltaic sand and gravel deposits (units Qvru1, Qvru2) is gradational.

We mapped subdued landslide-like features near the East Fork Union River at elevations below the shoreline elevation of Lake Russell as sublacustrine landslides (unit Qvls). Similarly, we interpreted a fan-shaped deposit east of the East Fork to be a sublacustrine fan (unit Qvlf). Topography suggests that most material mapped as lake deposits in Haeussler and Clark (2000) is overlain by alluvium, and we show it on this map as unit Qa.

Interpretation of the DEM reveals scattered alluvial surfaces throughout the quadrangle that mostly form terraces, and these are cut into or mantled by Vashon-age recessional outwash graded to Lake Russell. Combining the sequences and locations of the terraces with probable drainage paths during ice retreat allows reconstruction of probable ice-front locations across the quadrangle (fig. 1). We assigned ages to the recessional terraces on the basis of their elevation: the highest recessional terraces in any one drainage must be the oldest in that drainage. We assumed that the coeval ice front was not too far east or north of any particular group of terraces; in other words, if none of this particular group of terraces can be identified farther upstream, then they were not formed there. If some of the mapped recessional outwash were deposited subglacially—though the flat top surfaces and adjacent cutbanks on many terraces argue against this—then the ice front could have been farther downstream than we have shown it.

The oldest recessional outwash graded to Lake Russell on this map occurs on a ridge above the Tahuya River on the west edge of the quadrangle (units Qvrw1, Qvrw2). West of the quadrangle, these deposits fill a sinuous channel that crosscuts the regional ice striations (fig. 1; Haugerud, 2009). This channel is a typical landform produced by subglacial erosion (Booth and Hallet, 1993). Outwash units Qvrw1 and Qvrw2 were deposited subglacially or shortly after the glacier retreated from the channel. Southeast of the Tahuya River, units Qvrs1, Qvrs2, and Qvrs3 also fill a sinuous channel, but one that parallels the regional ice striations. The glacier margin must have been very close to the channel's head or, more likely, this channel also is of subglacial origin. Units Qvrs1, Qvrs2, and Qvrs3 are truncated by younger outwash in the Tahuya River valley.

The most extensive terraces graded to Lake Russell (units Qvrt1–Qvrt7) are in and along Tahuya River and upper Big Beef Creek. Projecting terrace elevations onto a north-south vertical plane (fig. 2) facilitates separation and correlation of terrace levels. The almost continuous surface of Qvrt7 rises northward from the southwest border of the quadrangle to reach a broad divide at the head of the Tahuya River, at an elevation of about 490 ft (150 m), where it continues down along Big Beef Creek to a minimum elevation of about 400 ft (132 m). Older terraces (units Qvrt1–Qvrt6) show this same pattern at a higher level, albeit not continuously. These terraces appear to have been formed by meltwater draining south from the ice front near Sprague Pond and subsequently folded. Formation of the upper Big Beef Creek terraces by north-flowing drainage seems unlikely, because the ice front was far to the northeast and unable to supply meltwater to this area by the time upper Big Beef Creek was ice free. If the upper Big Beef Creek terraces were formed subglacially, their northward slope could be primary, but we expect subglacial channels to be undulating in profile and to lack distinct breaks in slope at the channel margins, unlike the smoothly sloped, sharply bounded surfaces of unit Qvrt7 and some of the older terraces (units Qvrt1–Qvrt4).

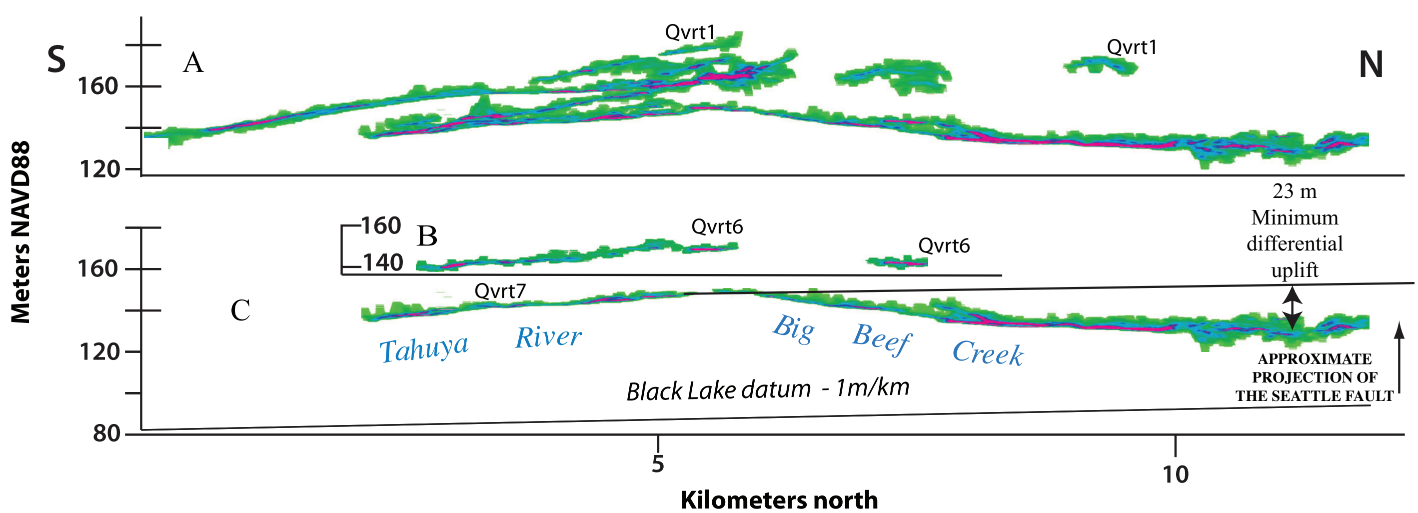

Figure 2. Profiles of deformed outwash terraces (Qvrt1–7) along Tahuya River and Big Beef Creek. Terrace DEM elevation points projected onto a north-south vertical plane. Frequency of elevation points are color coded: red, highest frequency. The spread of points vertically represents irregularities in terrace surface, inaccurate lidar data, and misidentification of terraces. *A*, composite plot of all Qvrt terrace surfaces (Qvrt1 labeled); *B* = Qvrt6; *C* = Qvrt7.

We discuss the significance of this young fold in the section on Structural History.

As the ice front retreated, it cleared the drainage of Bear Creek before the upper reaches of Union River and Hazel Creek were free of ice or a recessional lake. One prominent northeast tributary of Bear Creek grew to include upper Hazel Creek. Lower Hazel Creek was still ice covered, but after further retreat, lower Hazel Creek developed and was able to capture the upper headwaters of the Bear Creek tributary (fig. 1).

The exact origins of outwash terraces associated with lower Big Beef and Wildcat Creeks in the northeastern part of the quadrangle are somewhat problematic. After the ice receded from lower Big Beef Creek, the outwash drained through it to Hood Canal, depositing units such as Qvrb1–Qvrb3 (fig. 1). The outwash deposits of units Qvr1–Qvr3 could have formed subglacially as suggested by the sinuous channel draining into Lost Creek. When Chico Creek was free of ice, terraces Qvrc1–Qvrc2 could have been built.

Near McKenna Falls, on the southeast flank of Gold Mountain, recessional sediments (units Qvru1–Qvru2) form a delta that was built out into Lake Russell. Thorson (1989) calculated postglacial isostatic rebound at McKenna Falls to be about 161 ft (49 m) by subtracting the elevation of the Black Lake spillway (153 ft [46.7 m]) from the current elevation of the topset-foreset transition (314 ft [95.7 m]).

Post-glacial Deposits

Alluvial deposits mapped as Holocene and Pleistocene (unit Qoa) are scattered across the quadrangle. A sequence of terraces (units Qoa1–Qoa6) in Stavis Creek appears to have been graded to Pleistocene Lake Bretz. Small terraces in the canyon of Big Beef Creek may also have been graded to Lake Bretz. Note that terrace deposits are numbered sequentially within each drainage, thus Qoa1 in Stavis Creek may not be the same age as Qoa1 in Big Beef Creek.

The modern depositional environment includes alluvium (unit Qa), wetland deposits (unit Qw), and landslides (unit Qls). Holocene alluvium is clearly related to the modern drainage, but in some drainages mapped Holocene alluvium (unit Qa) may include some older alluvium (unit Qoa). Holocene alluvium is most extensive along the Union River and probably overlies lake deposits of Lake Russell. Many of the wetland deposits are perched on till, indicating that the till has poor drainage. Other wetlands, such as those surrounded by recessional outwash sand and gravel southwest of Tahuya Lake, appear to be filled with kettles that developed in contact with ice. A large alluvial fan (unit Qf1) built into Wildcat Lake on the southwest is traversed by a small scarp above a younger fan (unit Qf2), perhaps representing a change in lake level. Human modification of the topography is mostly seen as artificial fill (unit af) at the Olympic View Sanitary Landfill, near Barney White Ranch, and in road fill over low-lying areas.

Structural History

Sheeted dikes in the Green and Gold Mountains massif hint at structural conditions during their emplacement. Clark (1989) found that most dikes had north-northeast strikes and considerable variation in dike orientations (fig. 3). Paleomagnetic data from the Coast Range basalt terrain on the Olympic Peninsula indicates little rotation of the terrain in this latitude since emplacement of the dikes (Beck and Engebretson, 1982). Thus, their orientation suggests east-southeast to west-northwest extension during their emplacement, but perhaps the scatter in dike orientations indicates emplacement during a transtensional strain regime where σ1 or σ2 rotated about a vertical axis. A north-northeast-trending magnetic high in the aeromagnetic data (Blakely and others, 1999) parallels the trend of the most common dike orientation, suggesting that the dikes may contribute significantly to the aeromagnetic signature.

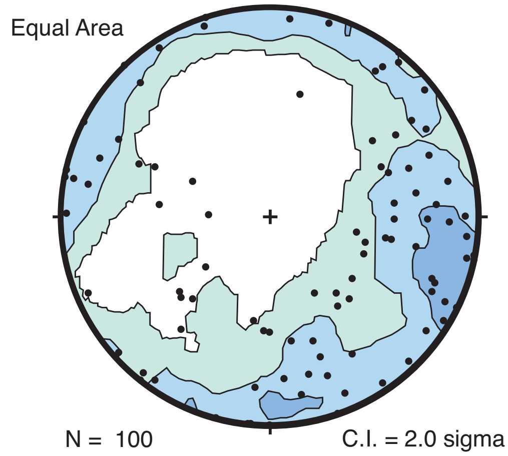

Figure 3. Kamb-contoured plot of poles to dikes of diabase and basalt. Black dots are poles to dikes. Data from Clark (1989).

The most significant fault in the quadrangle is the Seattle Fault, which extends along the south edge of the Seattle Basin from the east side of Lake Sammamish (east of Seattle) across Puget Sound to the Green and Gold Mountains area. On a regional scale, the sharpness of the gravity anomaly at the south side of the Seattle Basin, the presence of bedrock uplifts south of the Seattle Fault, such as Green and Gold Mountains, and the interpretation of seismic reflection and refraction data indicate that the Seattle Fault is a north-verging thrust (Johnson and others, 1994; Ten Brink and others, 2002). Johnson and others (1994) inferred that the Seattle Fault became active in late Eocene time. Ten Brink and others (2002) suggested that significant displacement on the Seattle Fault did not begin until Miocene time. An apatite fission-track date of 32±5 Ma from leucogabbro (Haeussler and others, 2000, also dated by U-Pb isotopes) is perhaps more consistent with initiation of movement on the Seattle Fault in early Oligocene time.

Prominent east-west valleys and offsets in quasi-ophiolitic layering led Clark (1989) to infer existence of the Tin Mine Lake Fault, which lies between the two lobes of Green Mountain, and the Gold Creek Fault, which lies between Green and Gold Mountains. Another roughly east-west-striking fault, which Haeussler and Clark (2000) refer to as the Holly Road Fault, is located along northwest Holly Road, just north of Green Mountain. The juxtaposition of submarine basaltic sediments (unit Tcbs) along the road with leucogabbro (unit Teg) on the north side of Green Mountain at its lowest elevations supports the placement of this fault. Similar strikes of the Seattle Fault, the Tin Mine Lake Fault, the Gold Creek Fault, the fault near the Union River Reservoir, and the Holly Road Fault suggest that these faults are related. Because the Seattle Fault is contractional, Clark (1989) inferred that the other east-west faults probably also are reverse faults. He inferred that the three northern faults are south dipping and that the Gold Creek Fault and fault near the Union River Reservoir are north dipping, but, with the exception of the Seattle Fault, the dip angles of all these faults are unconstrained.

Clark (1989) mapped three additional faults with northeast or north-northeast strikes. The Green Mountain Fault is a left-lateral oblique fault that bisects Green Mountain. Clark (1989) observed left-lateral slickensides on fault surfaces in outcrop. Offset of the quasi-ophiolitic layering indicates a northwest-side-down sense of dip-slip motion on the fault. On slickensided surfaces, the dip-slip slickensides are the youngest. A fault along Lost Creek, southeast of Green Mountain, has a strike and sense of separation similar to the Green Mountain Fault and is principally indicated by a geomorphic lineament and offset in the quasi-ophiolitic layering. A fault along the Union River, located north of the Union River Reservoir, follows a north-northeast-trending topographic lineament. West-side-up movement along this fault is indicated by offset of the quasi-ophiolitic layering.

Haeussler and Clark (2000) were uncertain how these northeast-striking faults relate to the east-west-striking faults. Clark (1989) concluded that the northeast-striking faults formed in the late stages of the same extensional event that produced the mafic dikes, on the basis of his inference that the dip-slip motion was normal and of the fault orientation. If these faults were normal, then the extension direction of the most common dike orientation is similar to the extension direction inferred by the faults. If the northeast-striking faults were related to dike intrusion, Heussler and Clark (2000) suggested that there should be faults that cut the lower, but not the entire, quasi-ophiolitic layering. Because they did not find such faults, they suggested that the northeast-striking faults could be related to contraction and (or) oblique motion on the Seattle Fault and related faults.

The overall structural pattern suggests north-south shortening after Crescent Formation time, a conclusion consistent with underthrusting of the Crescent Formation beneath Vancouver Island and with continued northward migration of the Coast Range in response to oblique subduction (Clowes and others, 1987; Wells and others, 1998).

Above, we discussed the evidence for folding of recessional outwash terraces (terrace Qvrt7) in the Tahuya River and Big Beef Creek valleys. This folding is younger than the ~16 ka age of the terraces. Projection of alluvial-plane elevations onto a north-south cross section and correction for 0.1 percent up-to-the north tilting by postglacial isostatic rebound (Thorson, 1989) closely defines a smooth fold with a 23-m-elevation difference between the low at Lake William Symington and the high at the Big Beef Creek-Tahuya River divide about 3 mi (5 km) to the southwest (fig. 2). Inclusion of the (unknown) paleogradient of the outwash stream increases the elevation difference.

We infer that this young fold is growing above the buried Seattle Fault (Haugerud and Tabor, 2008). The ~10-km width of the anticline is similar to the extent of uplift during the A.D. ~900 Seattle Fault earthquake farther east (ten Brink and others, 2006). The analysis of ten Brink and others (2006) suggests ~15 m of shortening during the A.D. 900 event that developed structural relief of ~9 m; scaling to the observed ≥23 m of relief observed in the Wildcat Lake quadrangle suggests ≥38 m of shortening in the last 16 ka, or ≥2 mm/yr. Booth and others (2004) estimated 0.5 mm/yr shortening on the Seattle Fault over the last several hundred thousand years.

DESCRIPTION OF MAP UNITS

UNCONSOLIDATED DEPOSITS

POSTGLACIAL DEPOSITS

af **Artificial fill (Holocene)**—Gravel, sand, soil, and broken rock. Includes concrete in dam at northeast end of Lake William Symington, fill along railroad near Twin Lakes and Leisureland Airpark, sanitary landfill near Barney White Ranch, and modified recessional outwash gravels and lake deposits

Qba **Alluvium (Holocene)**—Moderately sorted deposits of cobble gravel, pebbly sand, and floodplain sandy silt mostly along Stavis Creek, Big Beef Creek, and the Union River

Qls **Landslide deposits (Holocene)**—Diamicton of angular clasts of bedrock and surficial deposits derived from upslope commonly includes trees. Includes areas of irregular, hummocky topography. Poorly consolidated. Interpreted from the DEM

Qf **Alluvial fan deposits (Holocene and Pleistocene)**—Boulders, cobbles, and soft sand deposited in lobate form, where streams emerge from confining valleys and reduced gradients cause sediment loads to be deposited. Interpreted from the DEM. Locally divided by age

Qfy Younger alluvial fan (Holocene)

Qfo Older alluvial fan (Holocene and Pleistocene)

Qoa **Older alluvium (Holocene and Pleistocene)**—Moderately sorted deposits of cobble gravel, pebbly sand, and floodplain sandy silt. Located in several major drainages such as Union River and Stavis and Big Beaver Creeks. Divided from youngest to oldest

Qoa6 **Older alluvium, unit 6**

Qoa5 **Older alluvium, unit 5**

Qoa4 **Older alluvium, unit 4**

Qoa3 **Older alluvium, unit 3**

Qoa2 **Older alluvium, unit 2**

Qoa1 **Older alluvium, unit 1**

Qw **Wetland deposits (Holocene and late Pleistocene)**—Peat deposits with some intermixed sand, silt, and clay. Unit commonly occupies shallow depressions in till (unit Qvt) or low-lying areas of outwash (units Qvr, Qva)

GLACIAL AND INTERGLACIAL DEPOSITS

Deposits of Vashon stade of Fraser Glaciation of Armstrong and others (1965) (late Pleistocene)

Proglacial lake deposits

Qvrl **Recessional lacustrine deposits**

Qvlf **Recessional sublacustrine alluvial fan deposits**

Qvls **Recessional sublacustrine landslide deposits**

Qvro **Recessional outwash deposits**—Stratified and unconsolidated buff-colored sand and gravel deposits graded mostly to Lake Russell or, rarely, Lake Bretz. These deposits mostly form terraces mapped from youngest to oldest

Chico Creek outwash deposits—Two terraces graded to Lake Russell via Chico Creek

Qvrc2 **Chico outwash, unit 2**

Qvrc1 **Chico outwash, unit 1**

Big Beef Creek outwash deposits—Three terraces in a tributary to Big Beef Creek graded to Lake Bretz or Lake Russel via Big Beef Creek

Qvrb3 **Big Beef outwash, unit 3**

Qvrb2 **Big Beef outwash, unit 2**

Qvrb1 **Big Beef outwash, unit 1**

Outwash deposits south of Wildcat Creek—Three high terraces, which may have formed subglacially, graded to Lake Russell via Lost Creek

Qvr3 **Outwash, unit 3**

Qvr2 **Outwash, unit 2**

Qvr1 **Outwash, unit 1**

Tahuya River outwash deposits—In lower terraces in upper Big Beef Creek and Tahuya River, graded to Lake Russell via the Tahuya River

Qvrt7 **Tahuya outwash, unit 7**

Qvrt6 **Tahuya outwash, unit 6**

Qvrt5 **Tahuya outwash, unit 5**

Union Creek area outwash deposits—Graded to Lake Russell in Union Creek area, including a delta near Franklin Falls built into the lake

Qvru2 **Union Creek outwash, unit 2**

Qvru1 **Union Creek outwash, unit 1**

Big Beef-Tahuya-Mission outwash deposits—In higher terraces above upper Big Beef Creek, Tahuya River, and Mission Creek, graded to Lake Russell via south-draining creeks and rivers

Qvrt4 **Tahuya outwash, unit 4**

Qvrt3 **Tahuya outwash, unit 3**

Qvrt2 **Tahuya outwash, unit 2**

Qvrt1 **Tahuya outwash, unit 1**

Lower Tahuya River outwash deposits—Near west and southwest edge of quadrangle, graded to Lake Russell via lower Tahuya River

Qvrs3 **Southwest outwash, unit 3**

Qvrs2 **Southwest outwash, unit 2**

Qvrs1 **Southwest outwash, unit 1**

Qvrw2 **West outwash, unit 2**

Qvrw1 **West outwash, unit 1**

Qvri **Ice-contact deposits**—Stratified and unconsolidated buff-colored sand and gravel deposits with pitted outwash topography in southeastern part of map area. Sediments locally show deformation as a result of sag, slump, or collapse

Qvt **Till**—Compact light- to dark-gray, nonstratified diamict containing subangular to well-rounded clasts, glacially transported and deposited. Abundant granitic clasts were derived from Canada. Commonly overlies advance outwash deposits (unit Qva) and bedrock on Green and Gold Mountains. Forms undulating surface, with sediment less than 10 ft (3 m) to about 65 ft (20 m) thick (Deeter, 1978)

Qva **Advance outwash deposits**—Stratified to nonstratified gravel deposits. Locally consolidated and hard. Upper meter may be weathered buff to brown. Clasts are usually moderately to well rounded and <16 inches (<40 cm) across. Some deposits are diamicts that were deposited as debris flows issuing from front of advancing ice sheet. Debris-flow deposits in this unit are differentiated from till by (1) lack of clasts >16 in (>40 cm), (2) large cobbles commonly touching rather than matrix supported, (3) high proportion (roughly 40% or more) of large clasts, and (4) less compaction than till. As mapped, includes pre-Vashon-age deposits in Stavis Creek and probably in Big Beef Creek

Qpvu **Pre-Vashon-age deposits (Pleistocene)**—Glacial and interglacial sediments inferred to underlie oldest Vashon-age deposits. Shown on cross section only

BEDROCK

STRATIFIED ROCKS

Tb **Blakeley Formation (upper Eocene and Oligocene)**—Appears only in cross section, where it is inferred north of the Seattle Fault

Tcfv **Felsic volcanic(?) rock (middle Eocene)**—Fine-grained, pinkish-orange- to brown-weathering amygdaloidal quartz latite. Forms tabular bodies that could be either conformable interbeds or younger sills in submarine basalt. Probable high-level or extrusive equivalent of felsic intrusive rock, unit Tefv. Intergranular porphyritic or intergranular glomeroporphyritic; alteration minerals form about 50% of rock

Crescent Formation (middle Eocene)

Tcb **Massive basaltic lava flows**—Lavas contain pyroxene phenocrysts and calcite- or zeolite-filled amygdules. Texture in thin section is intergranular, with rock consisting of 45% labradoritic plagioclase, 35% augitic clinopyroxene, 15% opaques, and minor olivine and orthopyroxene. Individual flows are typically 10 m thick. Inferred to be subaerial because of a lack of interbedded sedimentary rocks. Exposed thickness is at least 590 ft (180 m) but may be more than 0.6 mi (1 km) (Clark, 1989)

Tcbs **Submarine basalt and related volcaniclastic rocks**—Dominantly greenish weathering submarine basalt flows interbedded with tuffs, tuff breccias, basaltic breccias, graded lithic and tuffaceous sandstones, basaltic siltstones, and conglomerates. No pillows recognized; vesicles are generally filled with calcite. In thin section, plagioclase typically composes about 50% of the rock, clinopyroxene 35%, and opaques about 10%. Sedimentary interbeds usually <1 m thick and as much as 10 m thick. These volcaniclastic rocks include altered lithic tuffs, volcanic breccias, aquagene crystal-lithic tuffs, graded basaltic sandstones and siltstones, and welded tuffs. Approximately 590 ft (180 m) thick. Intruded by dikes of basalt and diabase of unit Ted

INTRUSIVE ROCKS

Tad **Porphyritic and aphanitic dacite dikes (Eocene)**—Medium to light grey. Dikes cut all other bedrock units. In thin section, consists of about 50% plagioclase, 5–20% quartz, 10–15% amphibole, and about 15% other mafic minerals. Textures are, in decreasing abundance, pilotaxitic porphyritic, glomeroporphyritic with a felty groundmass, and hyalopilitic. Individual dikes shown on cross section only

Tefv **Felsic intrusive rocks (Eocene?)**—Quartz monzonite, quartz diorite, tonalite. Texture in thin section is intergranular granophyric. Intrudes basalts that appear to cut leucogabbro of unit Teg

Ted **Sheeted dikes of basalt and diabase (Eocene)**—Sheeted dikes are dark greyish black on fresh surfaces and weather bluish to greenish grey. Dikes are a few inches to 30 ft (10 m) thick but are most commonly about 3 ft (1 m) thick. Dike margins are chilled on either one or both sides. Textures range from very fine grained to diabasic and microgabbroic. Augite is dominant pyroxene in thin section. Dikes are amygdaloidal where they intrude the overlying submarine basalts and sediments. Zone consisting entirely of dikes is about 500 ft (150 m) thick. Individual dikes shown diagramatically on cross section only

Tegd **Leucogabbro and pegmatite intruded by dikes of basalt and diabase (Eocene)**—Leucogabbro and pegmatite, described in unit Teg, either fine or coarse grained, occur as screens between dikes of basalt and diabase. Dikes, of unit Ted, are as much as 30 ft (10 m) thick but are commonly about 3 ft (1 m) thick. Medium grey on fresh surfaces; weathers light gray to orange gray

Teg **Leucogabbro and pegmatite (Eocene)**—Massive leucogabbro, either fine or coarse grained. Medium grey on fresh surfaces; weathers light gray to orange gray. Texture in thin section is intergranular and glomeroporphyritic with phenocrysts of plagioclase and less commonly augitic pyroxene. Plagioclase ranges in composition from labradorite to bytownite. Overall rock composition is approximately 45% plagioclase, 40% clinopyroxene, as much as 5% brown hornblende, and 5% opaques. The brown hornblende is interstitial to other mineral phases. "Pegmatoid" denotes very coarse grained intrusive rocks associated with the leucogabbro. End members of the pegmatoid rocks are gabbroic and granophyric. Gabbroic pegmatoid rock has intergranular texture with ophitic to subophitic plagioclase grains to 1.5 in (3–4 cm) across. Rock composition is approximately 45% plagioclase, 40% clinopyroxene, and 5–10% magnetite. Granophyric pegmatoid rock is intergranular granophyric with grains to several centimeters across and an overall composition of 40% oligoclase, 10–20% pyroxene, 25% quartz, 10% micrographic regions, as much as 10% magnetite, and minor epidote and microcline

Teum **Ultramafic rocks (Eocene)**—Utramafic rocks beneath Green and Gold Mountains inferred from modeling aeromagnetic and gravity data. Rocks must be dense and magnetic. Shown only on cross section

References Cited

Armstrong, J.E., Crandell, D.R., Easterbrook, D.J., and Noble, J.B., 1965, Late Pleistocene stratigraphy and chronology in southwestern British Columbia and northwestern Washington: Geological Society of America Bulletin, v. 76, p. 321–330.

Arnold, Ralph, 1906, Geological reconnaissance of the coast of the Olympic Peninsula, Washington: Geological Society of America Bulletin, p. 451–468.

Atwater, B.F., and Moore, A.L., 1992, A tsunami about 1,000 years ago in Puget Sound, Washington: Science, v. 258, p. 1614–1617.

Babcock, R.S., Burmester, R.F., Engebretson, D.C., Warnock, A., and Clark, K.P., 1992, A rifted margin origin for the Crescent basalts and related rocks in the northern Coast Range volcanic province, Washington and British Columbia: Journal of Geophysical Research, v. 97, p. 6799–6821.

Beck, M.E., and Engebretson, D.C., 1982, Paleomagnetism of small basalt exposures in the west Puget Sound area, Washington, and speculation on the accretionary origin of the Olympic Moutains: Journal of Geophysical Research, v. 87, no. B5, p. 3755–3760.

Blakely, R.J., Wells, R.E., and Weaver, C.S., 1999, Puget Sound aeromagnetic maps and data: U.S. Geological Survey Open-File Report 99–514 (http://geopubs.wr.usgs.gov/open-file/of99-514).

Blakely, R.J., Wells, R.E., Weaver, C.S., and Johnson, S.Y., 2002, Location, structure, and seismicity of the Seattle fault zone, Washington—Evidence from aeromagnetic anomalies, geologic mapping, and seismic reflection data: Geological Society of America Bulletin, v. 114, no. 2, 169–177.

Booth, D.B., 1987, Timing and processes of deglaciation along the southern margin of the Cordilleran ice sheet, *in* Ruddiman, W.F., and Wright, H.E., Jr., eds., North America and adjacent oceans during the last deglaciation: Boulder, Colo., Geological Society of America, The geology of North America, v. K–3, p. 71–90.

Booth, D.B., and Hallet, B., 1993, Channel networks carved by subglacial water—Observations and reconstruction in the eastern Puget Lowland of Washington: Geological Society of America Bulletin, v. 105, p. 671–683.

Booth, D.B., Troost, K.G., and Hagstrum, J.T., 2004, Deformation of Quaternary strata and its relationship to crustal folds and faults, south-central Puget Lowland, Washington State: Geology, v. 32, no. 6, p. 505–508.

Brandon, M.T., Roden-Tice, M.K., Garver, J.I., 1998, Late

Cenozoic exhumation of the Cascadia accretionary wedge in the Olympic Mountains, northwest Washington State: Geological Society of America Bulletin, v. 110, p. 985–1009.

Brandon, M.T., and Vance, J.A., 1992, Tectonic evolution of the Cenozoic Olympic Subduction Complex, Washington State, as deduced from fission track ages for detrital zircons: American Journal of Science, v. 292, p. 565–636.

Bretz, J. Harlen., 1913, Glaciation of the Puget Sound region: Washington Geological Survey (State of Washington), Bulletin no. 8, 244 p.

Bucknam, R.C., Hemphill-Haley, Eileen, and Leopold, E.B., 1992, Abrupt uplift within the past 1700 years at southern Puget Sound, Washington: Science, v. 258, p. 1611–1614.

Clark, K.P., 1989, The stratigraphy and geochemistry of the Crescent Formation basalts and the bedrock geology of associated igneous rocks near Bremerton, Washington: Bellingham, Western Washington University, unpublished M.S. thesis, 171 p.

Clowes, R.M., Brandon, M.T., Green, A.G., Yorath, C.J., Sutherland Brown, A., Kanasewich, E.R., and Spencer, C., 1987, LITHOPROBE, southern Vancouver Island—Cenozoic subduction complex imaged by deep seismic reflections: Canadian Journal of Earth Sciences, v. 24, p. 31–51.

Deeter, J.D., 1978, Quaternary geology and stratigraphy of Kitsap County: Bellingham, Western Washington University, M.S. thesis, 175 p.

Dragovich, J.D, Logan, R.L., Schasse, H.W., Walsch, T.J., Lingley, W.S., Jr., Norman, D.K., Gerstel, W.J., Lapen, T.J., Schuster, J.E., and Meyers, K.D., 2002, Geologic Map of Washington—Northwest Quadrant: Washington Division of Geology and Earth Resources Geologic Map GM–50.

Duncan, R.A., 1982, A captured island chain in the Coast Range of Oregon and Washington: Journal of Geophysical Research, v. 87, p. 10,827–10,837.

Esser, R.P., 2003, $^{40}Ar/^{39}Ar$ Geochronology Results from two (Adakite) dikes from the Bremerton area of Washington: New Mexico Geochronology Research Laboratory Internal Report prepared for Dr. Jeff Tepper, Number NMGRL-IR-313, 7 p.

Garling, M.E., Molenaar, Dee, Bailey, E.G., VanDenburgh, A.S., Fiedler, G.H., 1965, Water resources and geology of the Kitsap Peninsula and certain adjacent islands: Washington Department of Water Resources, Water Supply Bulletin, p. 309.

Geomatrix Consultants, 1997, Conceptual hydrogeologic model report, Olympic View sanitary landfill: USA Waste Services, Inc., Kitsap County, Washington, Project No. 3946.

Gradstein, F.M., Ogg, J.G., and Smith, A.G., eds., 2004, A geologic time scale, 2004: Cambridge University Press, 585 p.

Haeussler, P.J., and Clark, K.P., 2000, Geologic Map of the Wildcat Lake 7.5′ quadrangle, Kitsap and Mason Counties, Washington: U.S. Geological Survey Open File Report 00-356, v. 1.0, scale 1:24,000.

Haeussler, P.J., Wells, R.E., Blakely, R.J., Murphy, John, and Wooden, Joe, 2000, Constraints on structure and timing of movement of the Seattle fault from structural geology, geophysics, and geochronology of the Green Mountain and Gold Mountain igneous complex, Washington: Geological Society of America Abstracts with Programs, v. 32, p. A–16.

Haugerud, R.A., 2009, Preliminary geomorphic map of the Kitsap Peninsula, Washington: U.S. Geological Survey, Open-File Report 2009–1033, 2 sheets, scale 1:36,000 (http://pubs.usgs.gov/of/2009/1033/).

Haugerud, R.A., Harding, D.J., Johnson, S.Y., Harless, J.L., Weaver, C.S., and B.L. Sherrod, 2003, High-resolution lidar topography of the Puget Lowland, Washington—A bonanza for earth science: GSA Today, v. 13, no. 6, p. 4–10.

Haugerud, R.A., and Tabor, R.W., 2008, Geomorphic evidence for multiple large post-glacial earthquakes on the Western Seattle Fault: American Geophysical Union, Fall Meeting 2008, abstract #T23E-05.

Jacoby, G.C., Williams, P.L., and Buckley, B.M., 1992, Tree ring correlation between prehistoric landslides and abrupt tectonic events in Seattle, Washington: Science, v. 258, p. 1621–1623.

Johnson, S.Y., Potter, C.J., and Armentrout, J.M., 1994, Origin and evolution of the Seattle fault and Seattle basin, Washington: Geology, v. 22, p. 71–74.

Karlin, R.E., and Abella, S.E.B., 1992, Paleoearthquakes in the Puget Sound region recorded in sediments from Lake Washington, U.S.A.: Science, v. 258, p. 1617–1620.

Porter, S.C., and Swanson, T.W., 1998, Radiocarbon age constraints on rate of advance and retreat of the Puget Lobe of the Cordilleran ice sheet during the last glaciation: Quaternary Research, v. 50, p. 205–213.

Pratt, T.L., Johnson, S.Y., Potter, C.J., Stephenson, W.J., Finn, C.A., 1997, Seismic reflection images beneath Puget Sound, western Washington State—the Puget Lowland thrust sheet hypothesis: Journal of Geophysical Research, v. 102, no. B12, p. 27,469–27,489.

Prothero, D.R., 2001, Magnetic stratigraphy of the middle Eocene Point of Rocks Sandstone (Ulatisian and type Narizian stages), western San Joaquin Basin, California, *in* Prothero, D.R., ed., Magnetic stratigraphy of the Pacific Coast Cenozoic: Society of Economic Paleontologists and Mineralogists, Pacific Section, v. 91, p. 65–74.

Reeve, William, 1979, Bedrock geology of the Blue Hills, Kitsap County, Washington: Golden, Colorado School of Mines, M.S. thesis, 58 p.

Sceva, J.E., 1957, Geology and groundwater resources of Kitsap County, Washington: U.S. Geological Survey Water Supply Paper 1413, 178 p.

Schuster, R.L., Logan, R.L., Pringle, P.T., 1992, Prehistoric rock avalanches in the Olympic Mountains, Washington: Science, v. 258, p. 1620–1621.

Snavely, P.D., Jr., MacLeod, N.S., and Wagner, H.C., 1968, Tholeiitic and alkalic basalts of the Eocene Siletz River Volcanics, Oregon Coast Range: American Journal of Science, v. 266, p. 454–481.

Spencer, P.K., 1984, Lower Tertiary biostratigraphy and paleoecology of the Quilcene-Discovery Bay area, northeast Olympic Peninsula, Washington: Seattle, University of Washington, Ph.D. dissertation, 173 p.

Tabor, R.W., and Cady, W.M., 1978a, Geologic map of the Olympic Peninsula, Washington: U.S. Geological Survey Miscellaneous Investigations Map I–994, scale 1:125,000, 2 sheets.

Tabor, R.W., and Cady, W.M., 1978b, The structure of the Olympic Mountains, Washington—Analysis of a subduction zone: U.S. Geological Survey Professional Paper 1033, 38 p.

Tabor, R.W., Haeussler, P.J., Haugerud, R.A., and Wells, R.E., 2011, lidar-revised geologic map of the Uncas 7.5′ quadrangle, Clallam and Jefferson Counties, Washington: U.S. Geological Survey Scientific Investigations Map 3160, 2 sheets, scale 1:24,000, pamphlet, 9 p., and GIS data.

ten Brink, U.S., Molzer, P.C., Fisher, M.A., Blakely, R.J., Bucknam, R.C., Parsons, T., Crosson, R.S., and Creager, K.S., 2002, Subsurface geometry and evolution of the Seattle fault zone and the Seattle basin, Washington: Bulletin of the Seismological Society of America, v. 92, p. 1737–1753.

ten Brink, U.S., Song, J., and Bucknam, R.C., 2006, Rupture models for the A.D. 900–930 Seattle fault earthquake from uplifted shorelines: Geology, v. 34, p. 585–588.

Tepper, J.H., Clark, K.P., Asmerom, Y., and McIntosh, W., 2004, Eocene adakites in the Cascadia Forearc—Implications for the position of the Kula-Farallon Ridge: Geological Society of America Abstract #72271, Rocky Mountain (56th Annual) and Cordilleran (100th Annual) Joint Meeting (May 3–5, 2004).

Thorson, R.M., 1979, Isostatic effects of the last glaciation in the Puget Lowland: Seattle, University of Washington, Ph.D. dissertation, 154 p.

Thorson, R.M., 1980, Ice-sheet glaciation of the Puget Lowland, Washington, during the Vashon Stade (late Pleistocene): Quaternary Research, v. 13, p. 303–321.

Thorson, R.M., 1989, Glacio-isostatic response of the Puget Sound area, Washington: Geological Society of America Bulletin, v. 101, p. 1163–1174.

Waitt, R.B., Jr., and Thorson, R.M., 1983, The Cordilleran ice sheet in Washington, Idaho, and Montana, *in* Porter, S.C., and Wright, H.E., Jr., eds., Late-Quaternary environments of the United States: University of Minnesota Press, v. 1, p. 53–70.

Weaver, C.E., 1937, Tertiary stratigraphy of western Washington and northwestern Oregon: University of Washington Publication in Geology, v. 4, 266 p.

Wells, R.E., Engebretson, D.C., Snavely, P.D., Jr., and Coe, R.S., 1984, Cenozoic plate motions and the volcano-tectonic evolution of western Oregon and Washington: Tectonics, v. 3, p. 275–294.

Wells, R.E., Weaver, C.S., and Blakely, R.J., 1998, Fore-arc migration in Cascadia and its neotectonic significance: Geology, v. 26, p. 759–762.

Willis, B., 1898, Drift phenomena of the Puget Sound: Geological Society of America Bulletin, v. 9, p. 111–162.

Willis, B., and Smith, G.O., 1899, Description of the Tacoma quadrangle, Washington: U.S. Geological Survey, Geological Atlas Folio, scale 1:125,000.

Yount, J.C., and Gower, H.D., 1991, Bedrock geologic map of the Seattle 30′ by 60′ quadrangle, Washington: U.S. Geological Survey Open-File Report 91–147, scale 1:100,000.

Yount, J.C., Minard, J.P., and Dembroff, G.R., 1993, Geologic map of surficial deposits in the Seattle 30′ by 60′ quadrangle, Washington: U.S. Geological Survey Open-File Report 93–233, scale 1:100,000.